SH 3.1.19

In Search of the Cosmic Ray Diffusion Tensor in the Heliosphere

J.P.L. Reinecke[1,3], F.B. McDonald[1], and H. Moraal[2]

[1] *Institute of Physical Science and Technology, University of Maryland,College Park, MD 20742, USA*

[2] *Space Research Unit, Potchefstroom University for CHE, Potchefstroom 2520, South Africa*

[3] *On sabbatical leave from the Potchefstroom University for CHE, Potchefstroom 2520, South Africa*

Abstract

In this paper we apply modulation models developed by the Potchefstroom Modulation Group to simulate as accurately as possible galactic hydrogen spectra measured over the past twenty-odd years especially during solar minimum modulation periods by various spacecraft. The goal is to learn as much as possible about the spatial and rigidity dependencies of the modulation tensor to complement the theoretical calculations of authors like Zank and coworkers (1998).

1 Introduction

The reason for continuing with our data fitting efforts after the publication of two rather lengthy papers (Reinecke et al., 1993 (no-drift paper) and 1996 (drift paper)) on this subject is that the diffusion tensors used in those papers had such a complex spatial dependence that it was almost impossible to interpret them physically.

All our previous solutions started with diffusion coefficients inversely proportional to the Parker spiral magnetic field strength, primarily because this choice seemed to work well, and also because it seemed logical. However, in order to fit the observations in detail, this Parker spiral magnetic field had to be modified drastically (see, for instance, Jokipii and Kota, 1989). These modifications were insufficient and additional, physically unjustified modifications had to be employed in the drift paper. These modifications were so drastic that this approach to fit the cosmic ray observations has become questionable.

2 Our present approach to data fitting

In a recent paper (Reinecke et al., 1997) we took a different approach by noting that according to the two-dimensional (r,q) cosmic ray transport equation the intensity f is explicitly determined by the effective radial and latitudinal diffusion coefficients κ_{rr} and $\kappa_{\theta\theta}$, or the corresponding effective diffusion mean free paths (dmfp's) λ_{rr} and λ_{qq}. In our present approach we specify λ_{rr} and λ_{qq} independent of a particular magnetic field and search for the simplest spatial dependence of λ_{rr} and λ_{qq} with which the observations can be fitted. The relationship between λ_{rr} and $\lambda_{\|}$, $\lambda_{\perp}$, the dmfp's parallel and perpendicular to the IMF is given by $\lambda_{rr} = \lambda_{\|} \cos^2 y + \lambda_{\perp} \sin^2 y$, where the spiral angle of the IMF is given by $\tan Y = (\Omega r \sin q)/V$ with Ω the angular speed of the sun and V the solar wind speed.

3 Model Details

For this paper we used the same time-independent $(\partial f/\partial t)$, two-dimensional modulation model employed in all our papers referred to above. All the dmfp's were chosen proportional to $b(P/P_o)$, where P is the particle rigidity and P_o = 1 GV. The solar wind speed increases smoothly from 400 km/s in the ecliptic plane to 750 km/s in the region between 5° and 60° above and below the ecliptic plane (Lima and Tsinganos, 1996). A simulated wavy current sheet was also included in the model. The galactic input spectrum for hydrogen was put at r_b = 120 AU and was the same one used by Reinecke et al. (1993).

To be able to modify the magnetic field above the solar poles, we chose (subscript e refer to values at Earth) $B = B_e(r_e/r)^2[(\cos y_e/\cos y)^2 + (d r/r_e)^{1/2]}$. When $\delta = 0$, this gives the standard Parker spiral field, while $\delta > 0$ corresponds to the polar modification suggested by Jokipii and Kota, and which have little effect in the ecliptic plane.

4 Results and discussion

4.1 1-D no-drift model: In our search for the simplest diffusion tensor which can account for the measurements, we start with a simple one-dimensional model with a spatially independent radial dmfp ($\lambda_{rr} = 0.5 \times P/P_o$ AU) and calculated solutions for both solar minimum polarity periods (Frame A1). The radial gradients in the inner heliosphere (r < 5 AU) are too small and in the outer heliosphere too large. The surprise is that the model very nearly fits the Voyager 1 data at 31 AU, 34^o N in 1987. This is due to the solar wind profile mentioned above, which is the only agent that causes a latitudinal dependence of the intensity, and which causes the latitudinal gradients to be sufficiently negative (solid lines, Frame A2) to account for the negative latitudinal gradient between V-1 and V-2 measured in 1987. It is the radial gradient that messes up this fit a bit. In Frame A3 intensities in the ecliptic plane for 120 and 1275 MeV protons are plotted as a function of the radial distance. The 1275 MeV intensity has a constant radial gradient of 0.52%/AU, which is exactly as expected from the Force-Field expression $g_r=CV/k_{rr}$. At 120 MeV the concave curvature of the radial intensity profiles is due to the increasing importance of adiabatic energy losses towards lower energies.

4.2 2-D no-drift models: The model solutions shown by broken lines in Frame A1 were calculated with a two-dimensional no–drift model for both polarity periods with the spatially independent dmfp's $\lambda_{rr} = 0.5 \times P/P_o$ AU; $\lambda_{qq} = 0.1 \times \lambda_{rr}$. For radial distances r < 50 AU this simple dmfp's do surprisingly well.

One sees that λ_{qq} has a significant effect in the inner heliosphere (r < 5 AU) and a very small effect for r > 30 AU. This is due to the fact that latitudinal diffusion is much more effective to relieve latitudinal gradients in the inner than in the outer heliosphere, because for a given gradient per unit of angle, the gradient per unit of distance decreases proportional to 1/r. This "ties" the intensities at the inner boundary into a single value as seen from the radial profiles plotted by broken in Frame A3. The latitudinal profiles shown by broken lines in Frame A2 show that $\lambda_{qq} > 0$ leads to very small latitudinal gradients in the inner heliosphere, precisely as has been observed by the Ulysses mission (Heber et al., 1996). The different sign of the latitudinal gradient observed by Ulysses does not invalidate the argument.

The fact that the calculated radial gradients in this simple 2-D model are too small in the inner heliosphere and too large in the outer heliosphere**,** suggests that λ_{rr} should increase with r in the inner heliosphere and decrease with r in the outer heliosphere.

The model solutions in Frame B1 were calculated with the mean free paths in Frame B2, plotted for 1 GV particles. Although not perfect, these are our best simultaneous fits yet to qA-positive and qA-negative measurements ranging from 1AU to 65 AU calculated with a single diffusion tensor. The solar wind profile discussed in the previous section causes the latitudinal gradients to be sufficiently negative to account for the negative latitudinal gradient between V-1 and V-2 measured in 1987. These negative gradients however cause the calculated spectrum for V-2 at 65.5 AU, 34^o N in 1997 to lie a bit lower than the measured values.

The radial dependence of the diffusion tensor in this figure is primarily determined by the radial distribution of the qA-positive (1977 and 1997) measurements. The qA-negative (1987) measurements can be adequately described with a no drift model in which λ_{rr} and λ_{qq} are spatially independent ($\lambda_{rr} = 0.467 \times P/P_o$ AU and $\lambda_{qq} = 0.1 \times \lambda_{rr}$).

4.3 Drift model solutions: The next step in our search for the simplest dmfp's was to add drifts to a model in which the dmfp's are independent of radial distance. In the case of the drift models it again turned out, as was the case in our drift paper, that one cannot simulate measurements made in the two polarity periods with the same dmfp's. We will therefore discuss the two cases separately.

4.3.1 qA<0 solar minimum period: The model solutions shown in Frame C1 were calculated with δ = 0.001 in the expression for B in Section 3. This imply that the magnetic field strenght above the poles at the modulation boundary was scaled down by a factor 24 in our model. The dmfp's were spatially independent

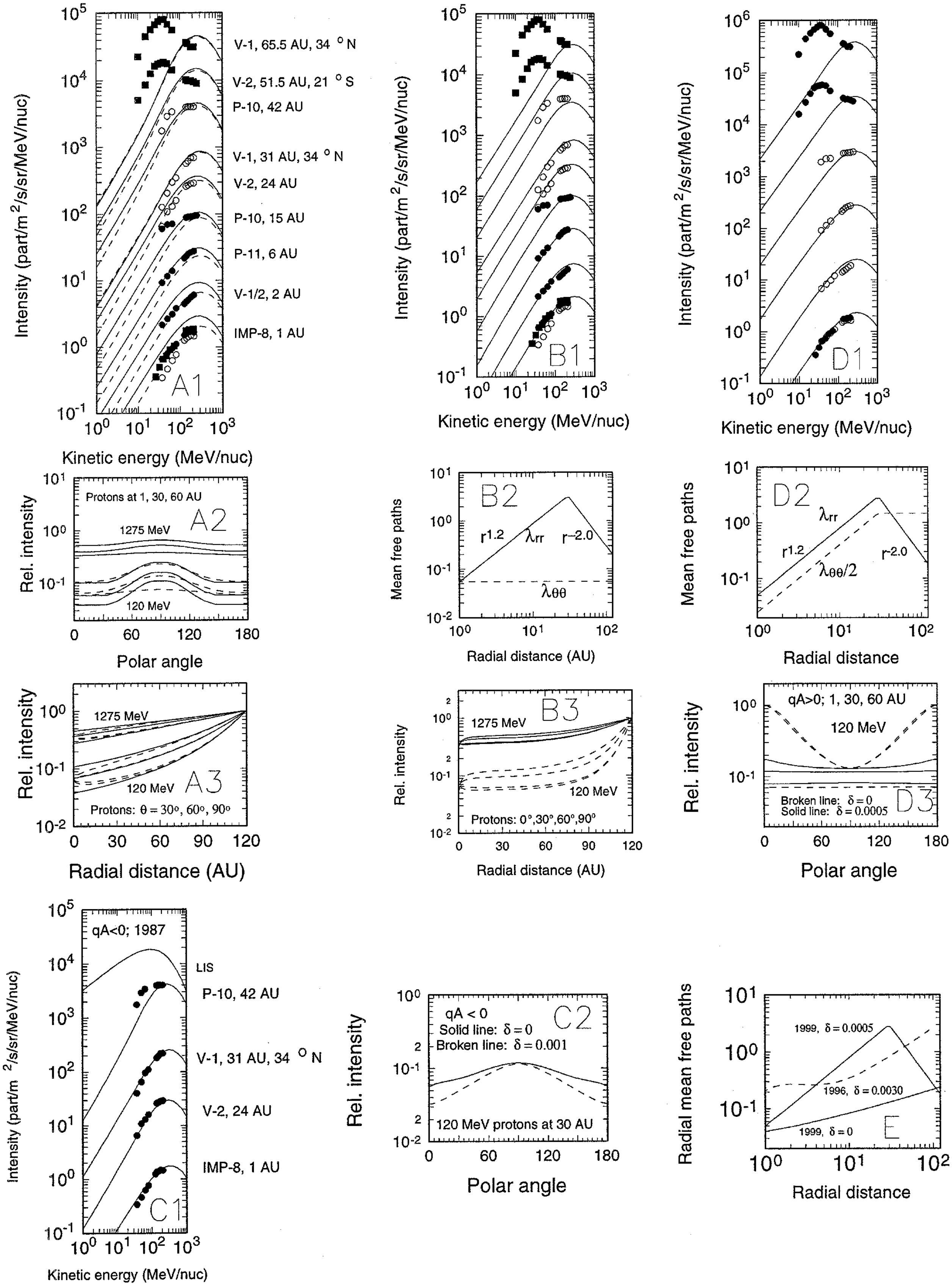

V-1, 65.5 AU, 34 °N
V-2, 51.5 AU, 21 °S
P-10, 42 AU
V-1, 31 AU, 34 °N
V-2, 24 AU
P-10, 15 AU
P-11, 6 AU
V-1/2, 2 AU
IMP-8, 1 AU
A1
Intensity (part/m²/s/sr/MeV/nuc)
Kinetic energy (MeV/nuc)
B1
D1
Protons at 1, 30, 60 AU
1275 MeV
120 MeV
A2
Rel. intensity
Polar angle
B2
Mean free paths
r1.2
λrr
r−2.0
λθθ
Radial distance (AU)
D2
λθθ/2
Radial distance
1275 MeV
120 MeV
A3
Protons: θ = 30°, 60°, 90°
Radial distance (AU)
B3
Protons: 0°,30°,60°,90°
qA>0; 1, 30, 60 AU
120 MeV
Broken line: δ = 0
Solid line: δ = 0.0005
D3
qA<0; 1987
LIS
P-10, 42 AU
V-1, 31 AU, 34 °N
V-2, 24 AU
IMP-8, 1 AU
C1
qA < 0
Solid line: δ = 0
Broken line: δ = 0.001
C2
120 MeV protons at 30 AU
Radial mean free paths
1999, δ = 0.0005
1996, δ = 0.0030
1999, δ = 0
E

($\lambda_{rr} = 0.275 \times P/P_o$ AU and $\lambda_{qq} = 0.10 \times \lambda_{rr}$). The effect of the field modification is to decrease intensities towards the solar poles as shown in Frame C2 where latitudinal intensity distributions are plotted as a function of polar angle for the unmodified field, $\delta = 0$, (solid line) and the modified field, $\delta = 0.001$ (broken line) at a radial distance of 30 AU. The enhancement in the negative latitudinal gradient is just sufficient to account for the V-1 intensities measured at 31 AU, 34^o N. This model is still very much drift dominated. If drifts are switched off, the intensity of 300 MeV protons at 1 AU decreases to 45% of its value with drifts switched on.

4.3.2 qA>0 solar minimum period: In the qA-negative modulation period it was necessary to modify the magnetic field above the poles. We therefore also included a similar modification ($\delta = 0.0005$) in this case. The calculated spectra shown in Frame D1 were calculated with the dmfp's shown in Frame D2 (plotted for 1 GV particles). The general agreement with the measurements is excellent. An important effect of the applied field modification is to cause the large positive latitudinal gradients at around 30 AU for the $\delta = 0$ case (broken lines), to be replaced with an almost zero gradients as shown by the solid lines in Frame D2. Because of this modified latitudinal gradients the fits to the 1997 V-1 and V-2 measurements are much better than fits calculated for an unmodified field.

5 Conclusions

In a no-drift model the solar wind profile causes a sufficiently negative latitudinal gradient at 30 AU in the 1987 qA-negative solar minimum modulation period to account for the V-1 spectrum at 31 AU, 34^o N. In a drift model however one has to employ an additional field modification above the solar poles to achieve this. In both cases the dmfp's were spatially independent.

For the qA-positive solar minimum modulation periods good drift model fits to the spectra in the ecliptic plane were achieved with no field modification and with diffusion mean free paths proportional to approximately $r^{1/2}$. To fit the V-1 spectrum at 65.6 AU, 34^o N in 1997 a small field modification had to be applied with a rather large effect on the radial dependence of diffusion mean free paths, especially in the outer heliosphere.

In Frame E the values for λ_{rr} for 1 GV particles are plotted as obtained from three drift models for the qA-positive modulation period, namely the model of our 1996 drift paper ($\delta = 0.003$), in which galactic hydrogen and helium spectra were simulated, and those of this paper with $\delta = 0$ (if one only consider measurements made in the ecliptic plane) and $\delta = 0.0005$. This illustrates that it is very difficult to find a unique radial dependence of λ_{rr}, even if one uses measurements at several radial distances.

Zank et al. (1998) have predicted in what they consider to be their physically most realistic model, that for 1 GV particles the radial dmfp λ_{rr} falls in the interval $0.1< \lambda_{rr} <0.2$ AU. The present data fits yields values for λ_{rr} (for 1 GV particles) in the range 0.55 (at 1 AU) - 3.0 AU (at 30 AU) from the model fits to the qA > 0 data sets and λ_{rr} (at 1 GV) = 0.275 from the drift model fits to the qA<0 data sets. All our values for λ_{rr} are therefore larger than the theoretical predictions.

References

Heber, B., et al. 1996, Astron. Astrophys., 316, 538
Jokipii, J.R., & Kota, J. 1989, Geophys. Res. Lett., 16, 1
Lima, J. & Tsinganos, K. 1996, Geophys. Rec. Lett., 23, 117
Reinecke, J.P.L., Moraal, H., & McDonald, F.B. 1993, J. Geophys. Res., 98, 9417
Reinecke, J.P.L., Moraal, H., & McDonald, F.B. 1996, J. Geophys. Res., 101, 21581
Reinecke, J.P.L., Moraal, H., Steenberg, C.D., & McDonald, F.B. 1997,
Zank, G.P., Matthaeus, W.H., Bieber, J.W. & Moraal, H. 1998, J. Geophys. Res., 103 2085